Influence of Monovalent Cations on Rat α- and β-Parvalbumin Stabilities†

Michael T. Henzl,* John D. Larson, and Sayeh Agah

Department of Biochemistry, University of Missouri—Columbia, Columbia, Missouri 65211

Received December 2, 1999; Revised Manuscript Received March 2, 2000

ABSTRACT: The mammalian genome encodes both α- and β-parvalbumin isoforms. The rat β-parvalbumin (aka "oncomodulin") is more stable than the α isoform at physiological pH and ionic strength, despite its substantially higher charge density and truncated C-terminal helix [Henzl, M. T., and Graham, J. S. (1999) *FEBS Lett. 442*, 241−245]. Reasoning that solvent interactions could contribute to this unexpected finding, we have examined the stabilities of the Ca^{2+}-free α- and β-parvalbumins as a function of Na^+ and K^+ concentration. Differential scanning calorimetry data suggest that, at physiological pH and ionic strength, the β isoform binds roughly 2 equiv of Na^+ or a single equivalent of K^+ with moderate affinity. Under comparable conditions, the α isoform apparently binds just 1 equiv of Na^+ and essentially no K^+. Isothermal titration calorimetry experiments suggest that the bound monovalent ions occupy the EF-hand motifs. In 0.15 M K^+, at pH 7.4, the stability of the apo-β-parvalbumin exceeds that of the α isoform by approximately 2.6 kcal/mol at 37 °C and by approximately 3.0 kcal/mol at 25 °C. The latter value represents a substantial fraction of the difference in Ca^{2+}-binding free energies measured in vitro for the two proteins. Significantly, however, these results do not completely explain the paradoxical stability of the β isoform, which maintains its higher melting temperature under all conditions examined.

Ca^{2+} plays a central role in eukaryotic signal transduction (*1*, *2*). Transient increases in cytosolic Ca^{2+} levels stimulate a broad spectrum of biological phenomena, ranging from muscle contraction to DNA transcription. Ca^{2+}−protein interactions pervade every aspect of the signaling process. The Ca^{2+} oscillations are produced by the action of channels and pumps in the endoplasmic or sarcoplasmic reticulum and plasma membrane; their amplitude and duration are further modulated by soluble Ca^{2+} buffer proteins; and their physiological consequences are dictated by an ever-expanding list of Ca^{2+}-dependent regulatory proteins. An appreciation of the kinetic and thermodynamic details of Ca^{2+} binding should, therefore, heighten our understanding of Ca^{2+}-dependent regulatory pathways.

Parvalbumins are small (M_r 12 000), vertebrate-specific EF-hand proteins that are believed to function as cytosolic Ca^{2+} buffers (*3* and references therein). They contain two canonical EF-hand motifs known as the CD and EF sites.[1] The parvalbumin (PV) family includes two sublineages, α and β, and mammals express one isoform from each lineage. Interestingly, both of these proteins have been detected in the sensory cells of the mammalian auditory organ, the organ of Corti: the α-PV is expressed by the inner hair cells (*4*, *5*) and the β-PV by the outer hair cells (*6*, *7*). Although the α isoform is present in other tissue settings (*8*)—notably fast-twitch muscle fibers and GABA-ergic neurons—the organ of Corti is apparently the sole site of expression for the β-PV in adult animals (*7*).

The rat α- and β-parvalbumins offer an attractive model system for exploring structure-function relationships in EF-hand proteins. For example, although the two proteins exhibit 49% sequence identity (Figure 1) and nearly identical peptide backbone conformations (*11*, *12*), the β-PV displays substantially lower affinity for Ca^{2+} and Mg^{2+} (*13*, *14*). A satisfactory explanation for this difference could improve our understanding of ion-protein structure-affinity relationships. However, despite a concerted effort by several laboratories, the issue remains unsettled.

Although influenced by the exact charge distribution, the electrostatic free energy of a protein roughly scales with the net charge (e.g., ref *15*). Being more acidic than their α counterparts, β-PVs (pI < 5) should therefore experience greater intramolecular electrostatic repulsion. Moreover, the abbreviated C-terminal helix in the β sublineage eliminates several favorable tertiary interactions (*12*, *16*). Given these considerations, it was surprising to learn that the Ca^{2+}-free rat β-PV [pI 3.9 (*17*)] displays a denaturation temperature significantly higher than that of the rat α-PV [pI 4.9−5.2 (*17*, *18*)] in 0.2 M NaCl at pH 7.4 (*19*). Differential interactions with solvent ions offered a potential explanation for this paradoxical behavior. Thus, we have undertaken a detailed investigation of parvalbumin conformational stability as a function of ionic strength and cation identity.

The influence of ionic composition on macromolecular stability is complex. At physiologically relevant concentra-

† This work was supported by NSF Award MCB9603877 (to M.T.H.). Portions of this work were presented at the 54th Calorimetry Conference, Tallahassee, FL, August 15−20, 1999, and at the Eleventh International Symposium on Calcium-Binding Proteins and Calcium Function in Health and Disease, Kisarazu, Japan, October 19−23, 1999.

* Corresponding author: Phone 573-882-7485; Fax 573-884-4812; e-mail henzlm@missouri.edu.

[1] Abbreviations: DSC, differential scanning calorimetry; ITC, isothermal titration calorimetry; EDTA, ethylenediaminetetraacetic acid; pI, isoelectric point; P_i, phosphate ion; PV, parvalbumin; CD site, parvalbumin metal ion-binding site flanked by the C and D helical segments; EF site, parvalbumin metal ion-binding site flanked by the E and F helical segments; GABA, γ-aminobutyric acid.

10.1021/bi992762g CCC: $19.00
Published on Web 04/21/2000

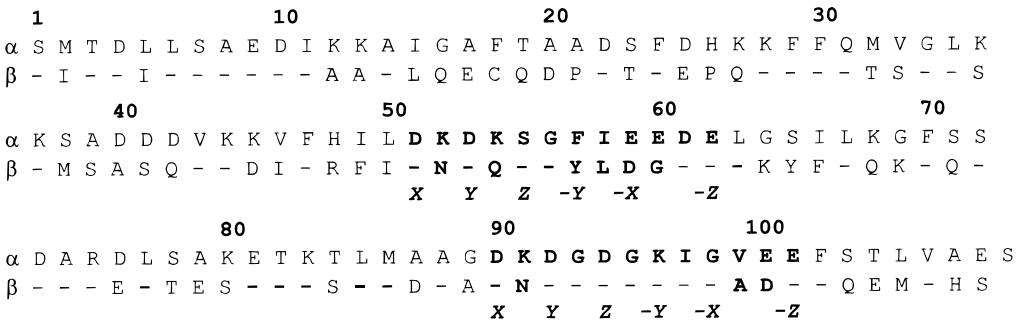

FIGURE 1: Sequence comparison of rat α- and *β*-parvalbumins. Data were obtained from Epstein et al. (*9*) and Gillen et al. (*10*), respectively. The CD (residues 50−62) and EF (residues 90−101) sites are displayed in boldface type. The coordinating ligands, positioned at the approximate vertexes of an octahedron, are designated *X*, *Y*, *Z*, −*Y*, −*X*, and −*Z*.

tions, solvent ions provide a counterion atmosphere that serves to attenuate coulombic interactions. In addition, solvent ions can function as discrete ligands, binding to defined regions of the protein molecule. Our data suggest that monovalent cations influence parvalbumin stability by both screening and site-specific binding and that the two mechanisms operate to differing extents in the two rat parvalbumin isoforms.

MATERIALS AND METHODS

All chemicals were analytical reagent-grade, purchased from Sigma−Aldrich Chemical Co. (St. Louis, MO) or Fisher Scientific Co. (Pittsburgh, PA).

Protein Purification. Purification schemes for the recombinant rat α- and *β*-parvalbumins have been described previously (*14*, *19*). Protein concentrations were determined spectrophotometrically, assuming $\epsilon_{258} = 1600\ M^{-1}\ cm^{-1}$ for the α isoform and $\epsilon_{274} = 3260\ M^{-1}\ cm^{-1}$ for the *β* isoform.

Both isoforms were homogeneous as judged by polyacrylamide gel electrophoresis, using Coomassie Blue for visualization. Furthermore, because both are devoid of tryptophan, their UV absorbance spectra provide a stringent test of purity. A_{280} should be negligible for the α-PV, given that phenylalanine is the sole aromatic chromophore. The material utilized for these studies was characterized by an A_{258}:A_{280} ratio greater than 20. Assuming an average extinction coefficient at 280 nm of 1 $(mg/mL)^{-1}\ cm^{-1}$ for protein contaminants, we estimate the heterogeneity of our α-PV preparations at less than 1%.

For the *β* isoform, which also contains tyrosine, the relative absorbance values at 274 and 290 nm provide an indication of purity. The material used for this work was characterized by an A_{274}:A_{290} ratio greater than 20. Assuming that half of the absorbance at 290 nm is due to contaminants and that the average extinction coefficient for protein contaminants at this wavelength is 0.5 $(mg/mL)^{-1}\ cm^{-1}$, we estimate the heterogeneity of our *β*-PV preparations at less than 2%.

When either PV isoform is titrated with Ca^{2+} ion in the titration calorimeter, the apparent stoichiometry is 2.0 ± 0.1. Moreover, the Ca^{2+}-binding enthalpies are very consistent from isolation to isolation. These findings suggest that microheterogeneity, arising from misfolding or chemical modification, is minimal in our parvalbumin preparations.

Calorimery. Differential scanning calorimetry (DSC) was performed with a modified Nano-DSC (Calorimetry Sciences Corp., Provo, UT), equipped with cylindrical sample cells. Excess EDTA was included in all samples to ensure that the proteins were present in their divalent ion-free forms. Both PV isoforms were observed to denature reversibly under the chosen experimental conditions (*19*). Samples were dialyzed to equilibrium against the reference buffer. Reference and sample cells were typically conditioned overnight with an aliquot of this buffer. In the morning, a baseline scan was acquired with fresh buffer, after which the protein sample was analyzed. Reference buffer solutions and protein samples were degassed under vacuum for 5 min prior to loading. We find that instrument performance is substantially improved by including a prerun, typically from 0 to 30 °C, in both the sample and baseline scans. Even with this precaution, we observe large variations in ΔH_d (see Figure 5). This uncertainty presumably arises from irreproducibility in the baseline and sample scans. Fortunately, most of our conclusions are based on alterations in transition temperature, which are extremely reproducible (± 0.2 °C). For applications requiring more precise estimates of the denaturational enthalpy, we averaged values from multiple experiments. All data analysis was performed with the CpCalc program (Applied Thermodynamics, Hunt Valley, MD).

The initial DSC samples were buffered solely by the EDTA ($pK_{a3} = 6.3$) used to maintain the parvalbumins in the Ca^{2+}-free state. Subsequent studies were performed in the presence of phosphate ion as well, to ensure adequate buffering. Inclusion of low concentrations of phosphate had no discernible impact on melting temperature.

Titration calorimetry was performed in a Calorimetry Sciences Corp. isothermal titration calorimeter. The enthalpies of tris(hydroxymethyl)aminomethane ionization (*20*) and chelation of Ba^{2+} by 18-crown-6 (*21*) were used for calibration and evaluation of instrument performance. Heat effects were integrated with DataWorks software (Applied Thermodynamics). Least-squares analyses of the integrated data were performed with BindWorks (Applied Thermodynamics). Parameter estimates represent the mean of at least three determinations; the stated uncertainty represents the maximal deviation from the mean.

Total cation levels were calculated by summing the chloride, phosphate, and EDTA contributions. The ionization states of phosphate and EDTA at pH 7.40 were determined by potentiometric titrations with standard NaOH. A total of 0.70 equiv of hydroxyl ion was required to raise the pH of 10 mM NaH_2PO_4 solution to 7.4, and 3.0 equiv was required to raise the pH of 10 mM EDTA (free acid) to 7.40. The cation contributions from these two species were thus

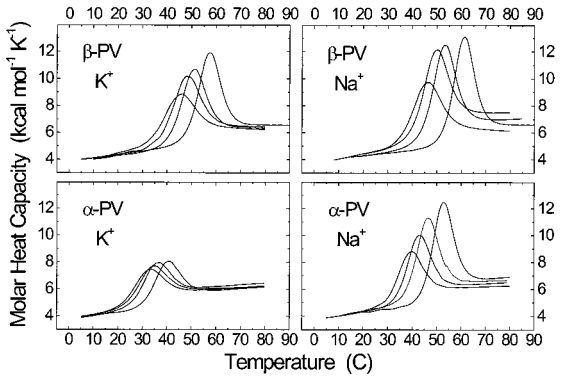

FIGURE 2: α- and β-PV stabilities are dependent on ionic composition. The melting temperatures of both proteins increase with increasing monovalent cation concentration. The samples employed for these analyses contained 5.0 mM phosphate, pH 7.4, 10 mM EDTA, and variable levels of the appropriate chloride salt: 0, 0.050, 0.20, or 1.0 M.

estimated by multiplying the total phosphate and EDTA concentrations by factors of 1.7 and 3.0, respectively.

Determinations of solvent-accessible surface area were performed with the NACCESS program (*22*), an implementation of the solvent-accessibility algorithm of Lee and Richards (*23*). The calculations utilized a probe radius of 1.4 Å and a slice width of 0.05 Å.

RESULTS

DSC Studies of PV Stability as a Function of Ionic Composition. PV conformational stability is strongly dependent on ionic composition, as indicated by the DSC scans shown in Figure 2. These data highlight several important issues. The melting temperatures (T_m) for both α- and β-PVs, as well as their denaturational enthalpy values, increase with Na^+ and K^+ concentration. However, the magnitude of the increase differs for the two proteins. Moreover, Na^+ is found to exert a greater stabilizing influence than K^+ on both proteins. Each of these topics is addressed in the following paragraphs.

Dependence of T_m on Monovalent Cation Concentration. The rat α- and β-PV isoforms were studied at pH 7.4 in the presence of Na^+ or K^+, at concentrations between 0.01 and 2.0 M. The α-PV T_m increases from 32 to 57 °C over this range; the β-PV T_m increases from 40 to 66 °C. Table 1 lists transition temperatures and calorimetric enthalpies for a subset of the experiments. Significantly, the β-PV maintains its greater stability under all conditions examined. We should emphasize, however, that this behavior is not representative of all β-PVs. For example, the carp (p*I* 4.25) β-PV exhibits a T_m of just 32 °C in 10 mM sodium phosphate and 5 mM EDTA, pH 7.5 (*24*)—stability comparable to that observed for the rat α-PV isoform.

Figure 3 displays the influence of cation concentration on melting temperature for the β (left) and α (right) isoforms. The distinct curves obtained with the Na^+ (●, ■) and K^+ (○, □) salts suggest the occurrence of specific cation effects. In the majority of these experiments, the chloride salts (●, ○) were used to adjust the monovalent cation levels. However, a subset of experiments employed phosphate as the major anion. Notice that the data collected at high sodium (■) or potassium (□) phosphate concentrations are not collinear with the chloride data, suggesting that PV stability is also influenced by anion identity, albeit to a lesser extent.

The hyperbolic curves obtained for the β isoform in both Na^+ and K^+, and for the α isoform in Na^+, are consistent

Table 1: DSC Data Summary

sample description[a]	T_m (°C)	ΔH_d (kcal/mol)
α-Parvalbumin, Na^+-Containing Buffers		
2.0 mM phosphate, 5 mM EDTA	37.7	43.9
2.0 mM phosphate, 5 mM EDTA	37.8	44.8
2.0 mM phosphate, 10 mM EDTA	38.9	51.7
2.0 mM phosphate, 10 mM EDTA	39.2	47.5
2.0 mM phosphate, 10 mM EDTA	38.9	48.8
10 mM EDTA	38.9	50.8
50 mM NaCl, 10 mM EDTA	42.4	55.7
100 mM NaCl, 10 mM EDTA	44.4	58.9
0.2 M NaCl, 10 mM EDTA	46.0	63.0
0.2 M NaCl, 10 mM EDTA	45.9	63.9
0.2 M NaCl, 10 mM EDTA	46.0	67.6
0.5 M NaCl, 10 mM EDTA	48.8	69.8
1.0 M NaCl, 10 mM EDTA	52.4	73.6
2.0 M NaCl, 10 mM EDTA	57.2	79.6
α-Parvalbumin, K^+-Containing Buffers		
5.0 mM phosphate, 10 mM EDTA	32.8	35.8
5.0 mM phosphate, 10 mM EDTA	32.8	34.3
10 mM EDTA	33.3	37.1
50 mM KCl, 5 mM phosphate, 10 mM EDTA	34.3	38.7
50 mM KCl, 5 mM phosphate, 10 mM EDTA	33.8	37.9
50 mM KCl, 10 mM EDTA	34.3	31.7
100 mM KCl, 10 mM EDTA	35.3	36.5
100 mM KCl, 10 mM EDTA	34.8	38.9
200 mM KCl, 5 mM phosphate, 10 mM EDTA	35.3	36.5
200 mM KCl, 5 mM phosphate, 10 mM EDTA	35.3	38.6
200 mM KCl, 5 mM phosphate, 10 mM EDTA	35.8	38.1
0.5 M KCl, 5 mM phosphate, 10 mM EDTA	37.6	36.9
0.5 M KCl, 5 mM phosphate, 10 mM EDTA	37.9	38.3
0.75 M KCl, 5 mM phosphate, 10 mM EDTA	39.2	39.4
0.75 M KCl, 5 mM phosphate, 10 mM EDTA	38.8	37.2
1.0 M KCl, 5 mM phosphate, 10 mM EDTA	40.2	38.8
1.0 M KCl, 5 mM phosphate, 10 mM EDTA	40.3	38.9
1.5 M KCl, 5 mM phosphate, 10 mM EDTA	42.7	40.7
2.0 M KCl, 5 mM phosphate, 10 mM EDTA	44.0	44.4
2.0 M KCl, 5 mM phosphate, 10 mM EDTA	44.3	42.7
2.0 M KCl, 5 mM phosphate, 10 mM EDTA	44.3	42.7
β-Parvalbumin, Na^+-Containing Buffers		
1.0 mM phosphate, 1 mM EDTA	41.1	48.5
1.0 mM phosphate, 2 mM EDTA	41.8	49.4
2.5 mM phosphate, 5 mM EDTA	43.6	59.5
5 mM phosphate, 10 mM EDTA	45.8	61.6
30 mM NaCl, 5 mM phosphate, 10 mM EDTA	48.1	70.6
60 mM NaCl, 5 mM phosphate, 10 mM EDTA	49.5	76.4
100 mM NaCl, 5 mM phosphate, 10 mM EDTA	50.3	78.4
120 mM NaCl, 10 mM phosphate, 5 mM EDTA	50.8	81.0 ± 2.0 (8)[b]
150 mM NaCl, 5 mM phosphate, 10 mM EDTA	52.2	82.3
200 mM NaCl, 5 mM phosphate, 10 mM EDTA	52.9	83.4
500 mM NaCl, 5 mM phosphate, 10 mM EDTA	56.9	88.2
750 mM NaCl, 5 mM phosphate, 10 mM EDTA	59.5	91.4
1.0 M NaCl, 5 mM phosphate, 10 mM EDTA	61.0	93.3
2.0 M NaCl, 5 mM phosphate, 10 mM EDTA	66.1	90.2
β-Parvalbumin, K^+-Containing Buffers		
1.0 mM KP_i, 1.0 mM EDTA	39.8	43.4
1.0 mM KP_i, 1.0 mM EDTA	39.8	43.2
1.0 mM KP_i, 2.5 mM EDTA	41.2	47.0
2.5 mM KP_i, 5.0 mM EDTA	43.1	51.0
5.0 mM EDTA	42.8	50.1
2.5 mM phosphate, 10 mM EDTA	45.1	56.0
2.5 mM phosphate, 10 mM EDTA	45.3	57.3
10 mM EDTA	44.8	51.3
20 mM EDTA	46.6	59.2
50 mM KCl, 10 mM EDTA	47.5	59.6
100 mM KCl, 5 mM phosphate, 10 mM EDTA	49.0	65.4
120 mM KCl, 10 mM phosphate, 5 mM EDTA	49.0 ± 0.2	72.5 ± 3.0 (10)
200 mM KCl, 10 mM EDTA	51.2	69.5
200 mM KCl, 5 mM phosphate, 10 mM EDTA	50.4	68.9
500 mM KCl, 5 mM phosphate, 10 mM EDTA	53.8	75.5
500 mM KCl, 10 mM EDTA	54.0	62.4
750 mM KCl, 5 mM phosphate, 10 mM EDTA	55.6	77.6
1.0 M KCl, 10 mM EDTA	57.2	75.3
2.0 M KCl, 10 mM EDTA	61.8	78.6

[a] The pH of each sample was adjusted to 7.40. [b] Number of replicates shown in parentheses.

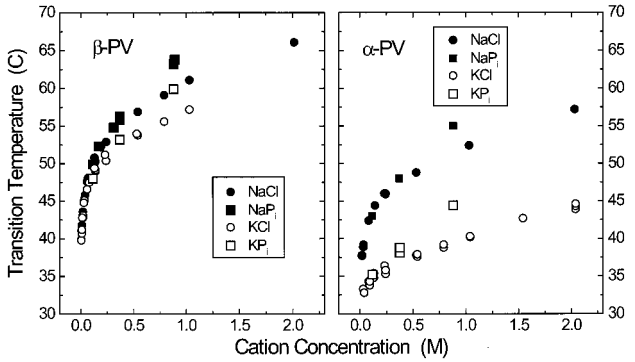

FIGURE 3: Dependence of melting temperature on cation concentration. Transition temperature is plotted versus monovalent cation concentration for DSC data collected on the β- (left) and α-PV (right) isoforms. Filled symbols (●, ■) denote data collected in Na^+-containing solution; open symbols (○, □) denote data collected in K^+. Circles (●, ○) denote experiments in which Cl^- was the major anion; squares (■, □) denote experiments in which phosphate (P_i) was the major anion.

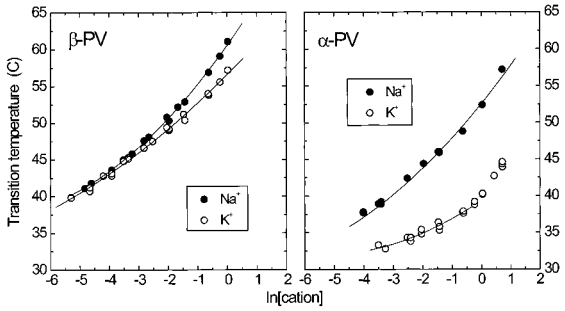

FIGURE 4: Apparent stoichiometry of cation binding. As described in the text, DSC data can furnish an estimate for Δn, the difference in cation-binding sites between the native and denatured states. The dependence of melting temperature on the natural logarithm of the cation concentration is shown in this figure for both β (left) and α (right) isoforms, in samples containing either NaCl (●) or KCl (○). The solid line through each data set represents the best least-squares approximation of the data by a quadratic equation.

with monovalent cation binding. These data can furnish an estimate for the number of cation binding sites or, more correctly, the difference in the number of binding sites (Δn) between the native and denatured states (e.g., refs *25*−*27*). Specifically,

$$\Delta n_M = [\Delta H_d/RT_m^2)(dT_m/d \ln(a_m)] \quad (1)$$

where ΔH_d is the calorimetrically measured enthalpy of denaturation, R is the universal gas constant, T_m is the melting temperature, and a_M is the thermodynamic activity of the monovalent cation. In Figure 4, T_m has been plotted versus ln [Na^+] and ln [K^+] for both rat parvalbumins. Due to the difficulty in obtaining accurate thermodynamic activity values, we have approximated activities with molar concentrations. These data sets were arbitrarily fit to quadratic equations, indicated by the solid lines through the points. The derivative of the fitting function provides an estimate for dT_m/d ln [M^+], which—when multiplied by $\Delta H_d/RT_m^2$—yields the value of Δn_M.

At a Na^+ concentration of 0.15 M, dT_m/d ln [Na^+] = 4.7 ± 0.2 for the β isoform. Substitution of this value into eq 1, together with a T_m of 324 K and ΔH_d of 81 kcal/mol, affords Δn_{Na} = 1.8 ± 0.2. The calculated value of dT_m/d ln [Na^+] for the α isoform at this concentration is 3.8 ± 0.2. This value, together with T_m of 318 K and ΔH_d of 59 kcal/mol, yields an estimate for Δn_{Na} of 1.1 ± 0.2. This analysis suggests that the β-PV binds somewhat more Na^+ than the α-PV at physiological pH and ionic strength.

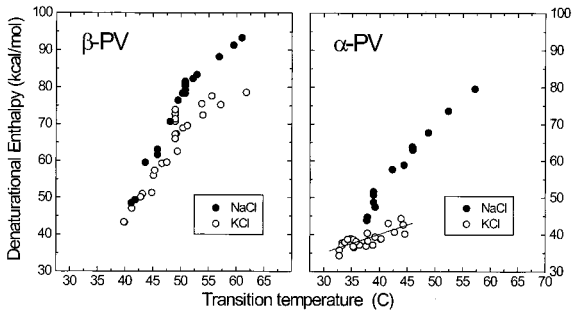

FIGURE 5: Dependence of ΔH_d on transition temperature. Denaturational enthalpy is plotted versus transition temperature for both β (left) and α (right) isoforms, in buffers containing either NaCl (●) or KCl (○). In principle, the slope of the plot equals ΔC_p for protein unfolding. This approach was used to estimate ΔC_p for α-PV in K^+. The solid line in the right panel represents the best linear fit to the data. Specific ion binding discouraged application of the method to the other three data sets. See text for details.

The α and β isoforms also differ with respect to K^+ binding. For the β-PV at a K^+ concentration of 0.15 M, dT_m/d ln [K^+] = 3.2 ± 0.2. With a T_m of 322 K and ΔH_d of 72 kcal/mol, we calculate a Δn_K = 1.1 ± 0.1, consistent with the binding of a single equivalent of K^+. By contrast, dT_m/d ln [K^+] = 1.6 ± 0.1 for the α-PV in 0.15 M K^+. With a T_m = 308 K and ΔH_d = 35 kcal/mol, Δn_K = 0.3 ± 0.1. Thus, the α-PV has little, if any, specific affinity for K^+ at physiologically relevant concentrations. The increase in slope observed at higher levels of the ion (Figure 4, right, ○) may, however, reflect the onset of binding to a low-affinity site.

Any doubts that we are witnessing the impact of specific ion-binding events are dispelled by the dissimilar effects of Na^+ and K^+ on α-PV stability. Whereas the T_m of the α isoform is 35 °C in 0.24 M K^+, it is 46 °C in 0.24 M Na^+. This difference contrasts the increase in stability resulting from site-specific ion binding with that resulting from mere electrostatic screening effects.

As expected, the Na^+ and K^+ data sets for either isoform show signs of converging at very low cation concentrations (Figure 4). By contrast, the behavior of the β-PV shows no indication of converging to that of the α-PV at zero cation concentration. The β-PV T_m remains 8 °C above the α-PV T_m at the lowest cation concentration examined. This result strongly suggests that differential solvent ion interactions are not entirely responsible for the superior stability of the rat β-PV isoform.

Denaturational enthalpy (ΔH_d) values have been plotted as a function of melting temperature for both rat parvalbumins in Figure 5. Judging from the difference between the Na^+ and K^+ data sets obtained with the α isoform (right panel), monovalent cation binding has a pronounced structural impact. The steep increase in ΔH_d with Na^+ concentration is indicative of a substantial conformational change and concomitant increase in van der Waals contacts. Although the β-PV ΔH_d values are perceptibly larger in Na^+ than in K^+ (left panel), the difference is not large, further suggesting that the conformational alteration is largely complete with binding of a single ion.

Table 2: Thermodynamic Parameters for Rat PV Denaturation in 0.15 M K^+ at pH 7.4

protein	T_m (K)	$\Delta H_d(T_m)$ (kcal mol^{-1})	$\Delta S_d(T_m)$ (kcal mol^{-1} K^{-1})	$\Delta C_p(T_m)$ (kcal mol^{-1} K^{-1})
α-PV	308.0 ± 0.2	37.4 ± 3.7	0.121 ± 0.012	0.51 ± 0.09
β-PV	322.0 ± 0.2	72.5 ± 3.0	0.225 ± 0.010	1.37 ± 0.13

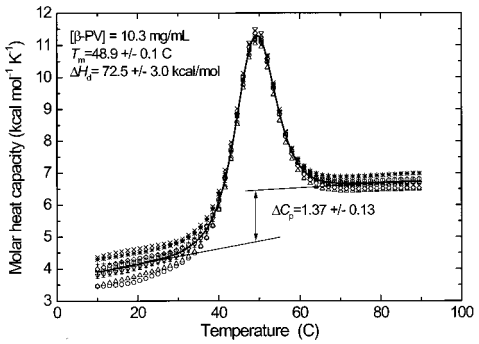

FIGURE 6: Determination of ΔC_p for unfolding of rat β-parvalbumin. DSC analyses were performed on 10 identical samples of the β isoform in 0.12 M KCl, 0.01 M phosphate, and 0.005 M EDTA, pH 7.40. For clarity, only a small subset of the data, every fifteenth point, is displayed. The solid line represents the average of the 10 replicates. ΔC_p was estimated from the difference between the extrapolated pre- and posttransition baselines at the melting temperature.

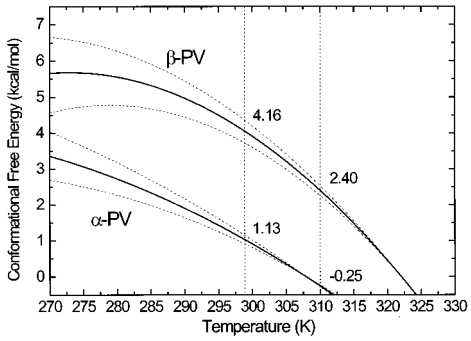

FIGURE 7: Conformational stability of the rat α- and β-parvalbumins. The solid lines were generated by substituting the parameter values listed in Table 2 into eq 2. The dashed lines were generated from the tabulated error estimates.

Relevant Conformational Stabilities of the Rat Parvalbumin Isoform. How do the stabilities of the Ca^{2+}-free α- and β-PVs compare under physiologically relevant conditions? This analysis requires estimates of ΔC_p for both proteins in 0.15 M K^+, pH 7.4. Since ΔC_p is the temperature derivative of ΔH_d, the slope of a plot of ΔH_d vs T_m should equal the ΔC_p for protein unfolding. We have utilized this relationship to obtain an estimate of ΔC_p for the α isoform in K^+ (Figure 5, right panel, ○). Linear regression (indicated by the solid line) yields a value for ΔC_p of 0.51 ± 0.09 kcal mol^{-1} K^{-1}. The potential interference of ion-binding phenomena in this type of analysis has been noted by others (e.g., refs *28* and *29*). Only the apparent absence of specific K^+ binding to the α isoform permitted application of this approach.

Since the β isoform binds K^+, the increase in ΔH_d attendant to an increase in [K^+] (Figure 5, left panel, ○) includes contributions from both cation dissociation and protein unfolding. Therefore, the slope of the ΔH_d vs T_m plot reflects the increasing occupation of the cation binding site as well as the temperature dependence of ΔH_d. The change in (ligation) state with increasing monovalent cation concentration may account for the apparent curvature of the plot, curvature that is even more evident in the Na^+ data set. We did not attempt to determine the β-PV ΔC_p from the ΔH_d vs T_m curve. In point of fact, the scatter in the data would likely have prevented a precise determination. Instead, an estimate of ΔC_p was extracted directly from the β-PV denaturation scans. These DSC experiments were performed with a protein concentration of 10.3 mg/mL, in 0.12 M KCl, 0.010 M phosphate, and 0.005 M EDTA, pH 7.4. The raw data are displayed in Figure 6. For the analysis, pre- and posttransition baselines were extrapolated into the transition region, and the difference between them was evaluated at the T_m. A linear function was used to model the pretransition baseline; a polynomial was used for the posttransition baseline. The average ΔC_p value, derived from 10 replicate experiments, was 1.37 ± 0.13 kcal mol^{-1} K^{-1}.

Two decades ago, Filimonov et al. (*24*) examined a β-PV isoform (p*I* 4.25) from carp by DSC and ITC. The ΔC_p value of 1.34 kcal mol^{-1} K^{-1} reported for the apoprotein was extracted from a plot of ΔH_d vs T_m obtained by varying Na^+ concentration. In light of the data presented here, it is likely that this ΔC_p value corresponds to the Na^+-bound form of the carp β-PV.

The values of T_m, $\Delta H_d(T_m)$, $\Delta S_d(T_m)$, and ΔC_p listed in Table 2 were substituted into (*30*)

$$\Delta G = \Delta H(T_m) - T\Delta S(T_m) + \Delta C_p[(T - T_m) - T \ln (T/T_m)] \quad (2)$$

to generate the stability curves shown in Figure 7. According to this analysis, which assumes that ΔC_p is temperature-independent, the rat α- and β-PVs differ in stability by 2.6 kcal/mol at 37 °C and by 3.0 kcal/mol at 25 °C.

Titration Calorimetry Studies of Na^+ and K^+ Binding to the Rat α and β-PV Isoforms. The interactions between Na^+ and K^+ and the two parvalbumin isoforms were also examined by isothermal titration calorimetry (ITC) at 25 °C, in 1 mM imidazole-EDTA, pH 7.40. The imidazolium/imidazole pair retains substantial buffering capacity at pH 7.40, and the size and geometry of the imidazolium cation should minimize competition with either Na^+or K^+ for specific binding sites on the proteins.

A representative titration of the β isoform with Na^+ is displayed in Figure 8A; corresponding data for K^+ are presented in Figure 8C. The integrated area under each peak represents the heat evolved with each addition of titrant. Although nonspecific contributions from titrant dilution are significant under these conditions, the heat fluxes observed in the presence of the protein (denoted by the thick lines) are substantially more exothermic than those observed with buffer alone (thin lines).

The integrated heats of binding, corrected for nonspecific mixing effects, are indicated by the open circles in Figure 9 panels A (Na^+) and B (K^+). These data were subjected to least-squares minimization—assuming the presence of *n* identical, independent sites—to obtain estimates for the enthalpies of binding and association constants. The value

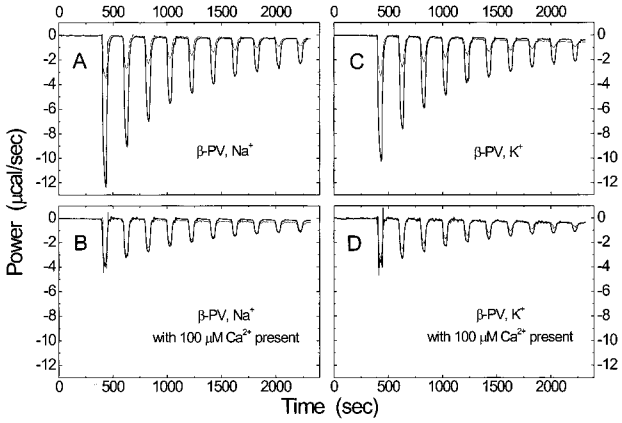

FIGURE 8: Titration of the β-PV with Na^+ or K^+; influence of Ca^{2+}. Rat β-PV (0.24 mM) was titrated with Na^+ or K^+ at pH 7.4, in 1.0 mM imidazole−EDTA (panels A and C) or in 3.0 mM imidazole, pH 7.4, containing 100 μM Ca^+ (panels B and D). Protein titrations are denoted by the thick black lines, buffer blanks by the thinner lines.

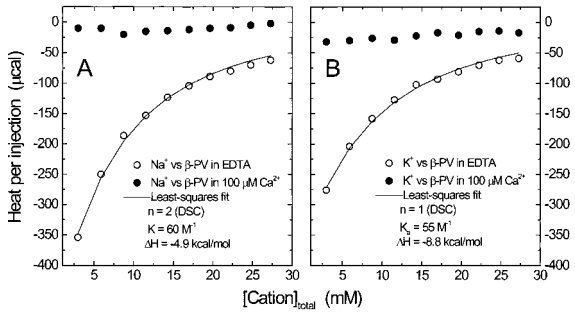

FIGURE 9: Analysis of monovalent cation binding to the β-PV. Heat released per injection is plotted vs total cation concentration for the ITC experiments shown in Figure 8. Open circles indicate data gathered in the presence of excess EDTA, and the solid lines indicate the best least-squares fit. Filled circles indicate data collected in the presence of 100 μM Ca^{2+}. (A) Titration with Na^+. Data collected in the presence of EDTA were modeled with the assumption of two identical sites, consistent with the DSC results. (B) Titration with K^+. Data collected in EDTA were modeled with the assumption of a single site.

of n was fixed for these analyses at the value suggested by the DSC analysis—2.0 for Na^+ and 1.0 for K^+. The solid lines in the figures represent the best fit to the experimental points. For Na^+, the best agreement between the calculated and observed values is obtained with $\Delta H_{Na} = -4.9 \pm 0.3$ kcal/mol and $K_{Na} = 60 \pm 10$ M^{-1}. Although the assumption of identical, independent binding sites may be simplistic, the small size of the data set prevents exploration of more complex models. For K^+, optimal agreement was achieved with $\Delta H_K = -8.8 \pm 0.4$ kcal/mol and $K_K = 55 \pm 8$ M^{-1}.

Parallel titrations of the β-PV with Na^+ and K^+ were also conducted in 3.0 mM imidazole, pH 7.40, containing 100 μM Ca^{2+}, at 25 °C. The raw data are presented in Figure 8 panels B and D, respectively. As above, the thinner lines correspond to titrations of buffer alone. The integrated data, corrected for nonspecific effects of titrant addition, are indicated by the filled circles (●) in Figure 9 panels A (Na^+) and B (K^+). It is apparent that the inclusion of low levels of Ca^{2+} virtually eliminates Na^+ and K^+ binding.

Representative titrations of the α-PV with Na^+ and K^+—likewise performed in 1 mM imidazole-EDTA, pH 7.40—are displayed in Figure 10 panels A and B, respectively. The Na^+ data qualitatively resemble those obtained with the β isoform. However, consistent with the scanning calorimetry data, the heat effects obtained by titrating the α-PV with K^+ (Figure 10B, thick line) were not significantly different from the titration of buffer alone (Figure 10B, thin line).

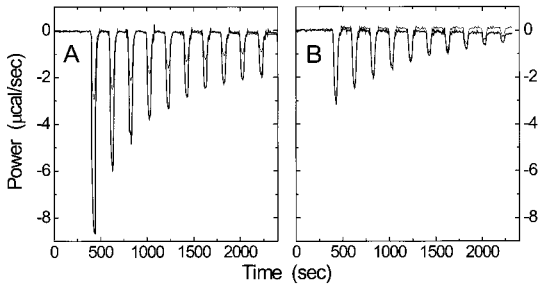

FIGURE 10: Titration of α-PV with Na^+ and K^+. Rat α-PV (0.25 mM) was titrated with 0.30 M Na^+ (panel A) or K^+ (panel B) at pH 7.4, in 1.0 mM imidazole−EDTA. Protein titrations are indicated by the thick black lines, buffer blanks by the thinner lines. Notice that the heats released per injection in the K^+ titration are comparable to those observed with buffer alone.

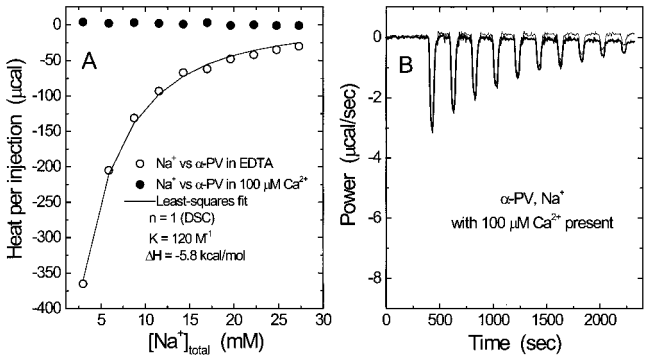

FIGURE 11: ITC analysis of Na^+ binding to α-PV: least-squares minimization and influence of Ca^{2+}. (A) Least-squares analysis of Na^+ binding. Open circles denote data collected in the absence of free Ca^{2+}. The solid line indicates the best fit obtained with the assumption of a single binding site. Filled circles correspond to the data, shown in panel B, collected in the presence of 100 μM Ca^{2+}. (B) Rat α-PV (0.25 mM) was titrated with 0.30 M NaCl in 5.0 mM imidazole, pH 7.40, containing 100 μM Ca^{2+}. The heat released upon titration of the protein (thick line) is comparable to that observed with buffer alone (thinner line), suggesting that inclusion of Ca^{2+} prevents Na^+ binding.

The integrated Na^+ titration data—after subtraction of the buffer blank—were subjected to least-squares analysis, with the assumption of a single binding site (Figure 11A). Optimal agreement between calculated and observed values was achieved with $K_{Na} = 120 \pm 10$ M^{-1} and $\Delta H_{Na} = -5.8 \pm 0.3$ kcal/mol. As observed for the β isoform, inclusion of low levels of Ca^{2+} abolishes the putative Na^+ binding event (Figure 11B).

DISCUSSION

Despite its higher charge density and shorter C-terminal helix, the Ca^{2+}-free form of the rat β-PV denatures at a higher temperature than the rat α-PV (*19*). Seeking an explanation for this unanticipated finding, we have examined the impact of ionic composition on parvalbumin stability. The implications of our data are discussed in the following paragraphs.

Monovalent Cation-Binding Behavior. The two rat parvalbumins display distinct monovalent cation-binding prop-

erties. DSC analyses suggest that, at physiologically relevant concentrations, the β-PV binds approximately 2 equiv of Na^+ or a single equivalent of K^+. Under comparable conditions, the α-PV binds a single equivalent of Na^+ and a mere fraction of an equivalent of K^+.

The DSC findings are corroborated by ITC experiments conducted at 25 °C. Titrations of the β isoform in excess EDTA, with either K^+ or Na^+, are accompanied by substantial release of heat. Least-squares analysis of the Na^+ data—assuming the existence of two equivalent binding sites—affords estimates for the binding constant and binding enthalpy of 60 M^{-1} and −4.9 kcal/mol, respectively. Analysis of the K^+ data, assuming just a single site, yields corresponding values of 55 M^{-1} and −8.8 kcal/mol.

Qualitatively similar behavior is observed when the α-PV is titrated with Na^+. Least-squares analysis indicates that the single ion is bound with an affinity of 120 M^{-1} and an enthalpy change of −5.8 kcal/mol. By contrast, when the α-PV is titrated with K^+, the resulting heat effects are comparable to those observed upon titration of buffer alone. Thus, DSC and ITC data both suggest that the rat α-PV has little affinity for K^+.

Identification of the Monovalent Cation Sites. Importantly, the heat effects that signal binding of Na^+ or K^+ are abolished by inclusion of 100 μM Ca^{2+} in the ITC samples, implying that the monovalent ions are bound within one or both EF-hand motifs. It should be noted that there is precedence for this type of behavior. Haiech et al. (*31*), for example, concluded that the EF-hand motifs in calmodulin bind K^+ competitively.

The divergent metal ion-binding properties of the rat α- and β-PV isoforms facilitate a tentative assignment of the monovalent ion sites. In considering this issue, we were influenced by the systematic lanthanide ion-binding studies of Sykes and colleagues (*32*−*34*). Their data revealed the nonequivalence of the parvalbumin CD and EF sites with respect to cation binding (*32*, *33*) as well as the differing behaviors of the rat α and β isoforms (*34*).

The EF sites are functionally similar in the rat α- and β-PV isoforms. The Ca^{2+} dissociation constants, for example, are 10 and 40 nM, respectively, in 0.15 M NaCl at pH 7.4. Accordingly, we suggest that either protein is capable of binding Na^+ within the EF site and that, in fact, the single equivalent of Na^+ bound by the α-PV occupies the EF site.

By contrast, the CD sites in the two proteins are functionally dissimilar. For example, the Ca^{2+} dissociation constants in 0.15 M NaCl at pH 7.4 are roughly 10 and 800 nM for the α and β isoforms, respectively. It is therefore likely that the lone equivalent of K^+ ion and the second equivalent of Na^+ bound by the β isoform occupy the CD binding site. These assignments should be regarded as preliminary, and experiments to test them are in progress.

Differential Impact of Na^+ and K^+ on α-PV Stability. Whereas the T_m of the α isoform is just 35 °C in 0.24 M K^+ at pH 7.4, it is 46 °C in 0.24 M Na^+. The disparate effects of K^+ and Na^+ on α-PV stability contrast the influence of simple electrostatic screening (K^+) and that due to specific ion binding (Na^+). Moreover, the pronounced impact of Na^+ binding in just one of the two EF-hand motifs also suggests that electrostatic destabilization is concentrated in the region of the ion-binding sites, consistent with the clustering of negatively charged side chains in the binding loops. This conclusion supports the contention by Williams et al. (*35*) that the parvalbumin denaturation reaction is driven by coulombic repulsion between the anionic ligands in the CD and EF loops.

Parenthetically, the differential stabilizing influence of K^+ and Na^+ explains the conflicting literature estimates of rat α-PV stability (*19*, *35*). In their NMR analysis of the α isoform, Williams et al. (*35*) determined a T_m of 35 °C and concluded that roughly 15% of the protein existed in the denatured form at 25 °C. By contrast, we observed a T_m for the rat α-PV of 46 °C (*19*). It is now clear that this discrepancy resulted from differences in solvent conditions. Whereas our initial estimate of the T_m was obtained in 0.20 M NaCl, the NMR work was carried out in 200 mM KCl. Under comparable conditions, we likewise measure a T_m of 35 °C. This observation underscores the importance of ionic composition on EF-hand protein structure and function and emphasizes the need for caution when discussing the properties of "apo" EF-hand proteins.

α- and β-PV Stability in Physiological Saline. The Ca^{2+}-free α and β isoforms differ appreciably in stability under pseudo-intracellular solution conditions, i.e., 0.15 M K^+ ion, pH 7.4. Using values of T_m, $\Delta H_d(T_m)$, $\Delta S_d(T_m)$, and ΔC_p from the DSC analyses (Table 2), we generated the stability curves displayed in Figure 7. At 37 °C, the β-PV is approximately 2.6 kcal/mol more stable than the α isoform. This difference increases to 3.0 kcal/mol at 25 °C. We hasten to add that this analysis, which neglects the decided influence of Mg^{2+}, is intended solely for discussion of in vitro data. Under actual physiological conditions, the α isoform will reside almost exclusively in the Mg^{2+}- or Ca^{2+}-bound form. The β-PV EF site will likewise be occupied primarily by Mg^{2+} or Ca^{2+} in vivo.

Monovalent cation binding contributes substantially to the superior stability of the β isoform. Substituting our estimate of 55 M^{-1} for the K^+ association constant into the relationship $\Delta G = -RT \ln K$, we calculate that roughly 2.4 kcal of that 3.0 kcal/mol difference in conformational stability at 25 °C derives from K^+ binding. This result suggests, however, that monovalent cation binding is not the sole stabilizing influence, consistent with our observation that the superior stability of the β isoform persists at low ionic strength.

Additional stabilizing factors apportion into two classes—those that raise the free energy of the β-PV denatured state and those that lower the free energy of its folded state. Concerning the former, we note that the β-PV sequence includes two proline residues, at positions 21 and 27, whereas the α sequence contains none. By decreasing conformational entropy, these substitutions should raise the free energy of the β-PV denatured state relative to that of the α. The substantially higher net charge on the β-PV might likewise influence the conformational entropy of the denatured state. Calculations on di- and tripeptides suggest that electrostatic interactions can modulate protein stability by perturbing the backbone conformational entropy (*36*).

Regarding stabilization of the folded β isoform, we note that 25 of the 55 sequence nonidentities between the α- and β-parvalbumins modify the net charge. Grimsley et al. (*37*) have recently shown that modulation of long-range coulombic interactions, by alteration of surface charges, offers a general mechanism for tuning conformational stability.

Their data suggest that charged ↔ neutral substitutions can provide on the order of 0.5 kcal/mol stabilization and that charge reversals can increase stability by more than 1.0 kcal/mol.

Impact of Ionic Composition on Divalent Ion-Binding Properties. Having tended to view the monovalent cations as "spectators" in our metal ion-binding studies of the rat β-PV, we were frankly surprised by the disparate monovalent cation-binding properties displayed by the two rat PV isoforms. When Eberhard and Erne reported that the rat α-PV binds Ca^{2+} and Mg^{2+} more tightly in the presence of K^+ than in Na^+ (*38*), we assumed that the β isoform would be similarly affected. However, our data suggest that the Ca^{2+}- and Mg^{2+}-binding properties of the two proteins will be differentially influenced by alterations in ionic composition. Whereas Na^+ ion competes with the divalent ions at just one of the α-PV sites, competition apparently occurs at both β-PV sites. And whereas K^+ is a bystander in binding studies on the α isoform, the ion can apparently compete with Ca^{2+} or Mg^{2+} at one of the β-PV sites. Studies are underway to more completely delineate the impact of monovalent cation concentrations on Ca^{2+} and Mg^{2+} affinities in these two proteins.

The rat β-PV is noteworthy for an attenuated affinity for divalent ions (*13*, *14*). The apparent $\Delta G°'$ for Ca^{2+}-binding represents the standard free energy change associated with this reaction:

$$\text{"apo-PV"} + 2Ca^{2+} \leftrightarrow Ca_2PV \qquad (3)$$

where the term "apo-PV" represents the Ca^{2+}-free parvalbumin, irrespective of monovalent cation ligation state. The contribution of free Ca^{2+} ion may be ignored in a comparison of the two PV isoforms because it will be identical for both, permitting us to focus on the relative energy difference between the "apo" and Ca^{2+}-bound states. A priori, a reduction in Ca^{2+} affinity, as seen for the rat β isoform, can be achieved either by stabilizing the Ca^{2+}-free form of the protein or by destabilizing the Ca^{2+}-bound form. The substantially greater stability of the β isoform in physiological saline (3.0 kcal/mol at 25 °C) suggests that the former mechanism contributes significantly to the observed reduction in divalent ion affinity observed in vitro (*13*, *14*).

Structural Implications. The large increases in denaturational enthalpy (ΔH_d) with cation concentration (Figure 5) and the substantial binding enthalpies observed during titrations with Na^+ or K^+ presumably reflect conformational adjustments in the polypeptide that result in more effective van der Waals contacts. In this respect, the parvalbumin behavior contrasts with that observed for α-lactalbumin − a small globular calcium-binding protein unrelated to the EF-hand family. Binding of Na^+ to lactalbumin does not produce a noticeable heat effect (*39*).

Whereas the α-PV metal ion-binding sites are unoccupied in K^+-containing buffers in excess EDTA, K^+ occupies one of the β-PV sites. This difference in ligation state produces a large difference in the apparent ΔC_p values: 0.51 kcal mol^{-1} K^{-1} for the α isoform, 1.37 kcal mol^{-1} K^{-1} for the β. The substantial increase in ΔC_p resulting from K^+ binding to the parvalbumin molecule highlights another contrast between the parvalbumin and α-lactalbumin systems. In the latter, the ΔC_p values for the apo- and monovalent cation-bound forms are reportedly indistinguishable (*39*).

The increase in protein heat capacity upon denaturation is primarily due to the concomitant increase in solvent-accessible apolar surface area. Thus, the large discrepancy in ΔC_p values for the rat α and β isoforms—0.51 and 1.36 kcal mol^{-1} K^{-1}, respectively—suggests that the Ca^{2+}-free forms of the two proteins are structurally dissimilar in K^+-containing buffers.

Several investigators have developed empirical methods for relating ΔC_p to changes in solvent accessible area (*40*−*43*). According to the Freire-Murphy formalism (*42*, *43*)

$$\Delta C_p = 0.45\Delta ASA_{ap} - 0.26\Delta ASA_{pol} \qquad (4)$$

$$\Delta H(60) = 31.4\Delta ASA_{pol} - 8.44\Delta ASA_{ap} \qquad (5)$$

where ASA_{pol} and ASA_{ap} are the changes in accessible polar and apolar surface area, respectively (in square angstroms), and $\Delta H(60)$ is the measured or extrapolated enthalpy change at 60 °C. For ΔC_p = 510 cal mol^{-1} K^{-1} and $\Delta H_d(60)$ = 51 000 cal mol^{-1} (extrapolated), we calculate that denaturation of the apo-α-PV is accompanied by exposure of 2280 and 2450 Å^2 of polar and apolar surface area, respectively. The corresponding values estimated from the crystal structure for the Ca^{2+}-bound protein (*12*) are 4130 and 6170 Å^2—an indication that the structure of the apoprotein in K^+ solution is substantially less compact than that of the Ca^{2+}-bound protein, with resultingly greater solvent penetration. This conclusion conflicts with the suggestion by Williams et al. (*35*) that the apo form of the rat α isoform adopts a conformation that is very similar to the divalent metal ion-bound forms.

Similar calculations for the β isoform, with ΔC_p = 1370 cal mol^{-1} K^{-1} and $\Delta H_d(60)$ = 88 000 cal mol^{-1}, suggest that roughly 5520 Å^2 of apolar surface and 4280 Å^2 of polar surface are exposed upon unfolding. These values approach those estimated for the crystal structure of the Ca^{2+}-bound protein (*11*), 5630 and 4040 Å^2, respectively, suggesting that the structure of the K^+-bound form of the rat β isoform approximates that of the Ca^{2+}-bound protein.

Concluding Remarks. DSC and ITC data indicate that the Ca^{2+}-free rat α- and β-parvalbumins differ significantly in their interactions with Na^+ and K^+. Whereas the β isoform binds roughly 2 equiv of Na^+ or a single equivalent of K^+ at physiologically relevant concentrations of the ions, the α isoform binds a single equivalent of Na^+ and essentially no K^+. The monovalent ions apparently occupy the EF-hand domains. Their binding provokes substantial conformational alterations, manifested in pronounced increases in ΔH_d with cation concentration, large binding enthalpies, and a substantial increase in ΔC_p.

Although Na^+ and K^+ preferentially stabilize the rat β-PV, the protein remains more stable than the α isoform at low ionic strength, suggesting the influence of additional stabilizing factors. At 25 °C, in 0.15 M K^+ at pH 7.4, the Ca^{2+}-free β-PV is an estimated 3.0 kcal/mol more stable than the α-PV. This enhanced stability of the β-PV, due in part to a more favorable interaction with monovalent ions, may contribute substantially to its reduced affinity for divalent ions.

Of course, the conclusion that increased competition from monovalent ions contributes to the attenuated affinity of the

rat β-PV for Ca^{2+} and Mg^{2+} raises additional questions. Foremost, what are the structural and energetic bases for the difference in monovalent ion affinities displayed by the rat α and β isoforms? Second, to what extent do monovalent cations shape the divalent ion-binding properties of other EF-hand proteins? Exploration of these issues should improve our understanding of metal ion-binding behavior in this physiologically important class of proteins.

REFERENCES

1. Meldolesi, J., and Pozzan, T. (1998) *Trends Biochem. Sci. 23*, 10−14.
2. Tsien, R. W., and Tsien, R. Y. (1990) *Annu. Rev. Cell Biol. 6*, 715−760.
3. Berchtold, M. W. (1996) in *Guidebook to the Calcium-Binding Proteins* (Celio, M., Pauls, T., and Schwaller, B., Eds.) pp 123−128, Oxford University Press, Oxford, England.
4. Eybalin, M., and Ripoll, C. (1990) *C. R. Acad. Sci. Paris 310*, 639−644.
5. Pack, A. K., and Slepecky, N. B. (1995) *Hear. Res. 91*, 119−135.
6. Sakaguchi, N., Henzl, M. T., Thalmann, I., Thalmann, R., and Schulte, B. A. (1997) *J. Histochem. Cytochem. 46*, 29−39.
7. Thalmann, I., Thalmann, R., and Henzl, M. T. (1998) *Prim. Sensory Neuron 2*, 283−296.
8. Heizmann, C. W. (1988) in *Calcium and Calcium Binding Proteins. Molecular and Functional Aspects* (Gerday, C., Bolis, L., and Gilles, R., Eds.) pp 93−101, Springer-Verlag, Berlin.
9. Epstein, P., Means, A. R., and Berchtold, M. W. (1986) *J. Biol. Chem. 261*, 5886−5891.
10. Gillen, M. F., Banville, D., Rutledge, R. G., Narang, S., Seligy, V. L., Whitfield, J. F., and MacManus, J. P. (1987) *J. Biol. Chem. 262*, 5308−5312.
11. Ahmed, F. R., Rose, D. R., Evans, S. V., Pippy, M. E., and To, R. (1993) *J. Mol. Biol. 230*, 1216−1224.
12. McPhalen, C. A., Sielecki, A. R., Santarsiero, B. D., and James, M. N. G. (1994) *J. Mol. Biol. 235*, 718−732.
13. Cox, J. A., Milos, M., and MacManus, J. P. (1990) *J. Biol. Chem. 265*, 6633−6637.
14. Hapak, R. C., Lammers, P. L., Palmisano, W. A., Birnbaum, E. R., and Henzl, M. T. (1989) *J. Biol. Chem. 264*, 18751−18760.
15. Tanford, C. (1961) *Physical Chemistry of Macromolecules*, pp 457−525, John Wiley & Sons, New York.
16. Padilla, A., Cavé, A., and Parello, J. (1988) *J. Mol. Biol. 204*, 995−1017.
17. MacManus, J. P., and Whitfield, J. F. (1983) *Calcium and Cell Function* (Cheung, W. Y., Ed.) pp 411−440, Academic Press, New York.
18. Berchtold, M. W., Wilson, K. J., and Heizmann, C. W. (1982) *Biochemistry 21*, 6552−6557.
19. Henzl, M. T., and Graham, J. S. (1999) *FEBS Lett. 442*, 241−245.
20. Christensen, J. J., Hansen, L. D., and Izatt, R. M. (1976) *Handbook of Proton Ionization Heats and Related Thermodynamic Quantities*, John Wiley & Sons, New York.
21. Briggner, L.-E., and Wadsö, I. (1991) *Biochem. Biophys. Methods 22*, 101−118.
22. Hubbard, S.J., and Thornton, J. M. (1993), NACCESS Computer Program, Department of Biochemistry and Molecular Biology, University College London.
23. Lee, B., and Richards, F. M. (1971) *J. Mol. Biol. 55*, 379−400.
24. Filimonov, V. V., Pfeil, W., Tsalkova, T. N., and Privalov, P. L. (1978) *Biophys. Chem. 8*, 117−122.
25. Alberty, R. A. (1969) *J. Am. Chem. Soc. 91*, 3899−3903
26. Plaza del Pino, I. M., and Sanchez-Ruiz, J. M. (1995) *Biochemistry 34*, 8621−8630.
27. Makhatadze, G. I., Lopez, M. M., Richardson, J. M., III, and Thomas, S. T. (1998) *Protein Sci. 7*, 689−697.
28. Lohman, T. M., Overman, L. B., Ferrari, M. E., and Kozlov, A. G. (1996) *Biochemistry 35*, 5272−5279.
29. McCrary, B. S., Bedell, J., Edmondson, S. P., and Shriver, J. W. (1998) *J. Mol. Biol. 276*, 203−224.
30. Becktel, W. J., and Schellman, J. A. (1987) *Biopolymers 26*, 1859−1877.
31. Haiech, J., Klee, C. B., and Demaille, J. G. (1981) *Biochemistry 20*, 3890−3897.
32. Corson, D. C., Williams, T. C., and Sykes, B. D. (1983) *Biochemistry 22*, 5882−5889.
33. Williams, T. C., Corson, D. C., and Sykes, B. D. (1984) *J. Am. Chem. Soc. 106*, 5698−5702.
34. Williams, T. C., Corson, D. C., Sykes, B. D., and MacManus, J. P. (1987) *J. Biol. Chem. 262*, 6248−6256.
35. Williams, T. C., Corson, D. C., Oikawa, K., McCubbin, W. D., Kay, C. M., and Sykes, B. D. (1986) *Biochemistry 25*, 1835−1846.
36. D'Aquino, J. A., Amzel, L. M., and Freire, E. (1999) *Biophys. J. 76*, A117.
37. Grimsley, G. R., Shaw, K. L., Fee, L. R., Alston, R. W, Huyghues-Despointes, B. M. P., Thurlkill, R. L., Scholtz, I. M., and Pace, C. N. (1999) *Protein Sci. 8*, 1843−1849.
38. Eberhard, M., and Erne, P. (1994) *Eur. J. Biochem. 222*, 21−26.
39. Griko, Y., and Remeta, D. P. (1999) *Protein Sci. 8*, 554−561.
40. Spolar, R. S., Livingstone, J. R., and Record, M. T. (1992) *Biochemistry 31*, 3947−3955.
41. Spolar, R. S., and Record, M. T. (1994) *Science 263*, 777−784.
42. Murphy, K. P., and Freire, E. (1992) *Adv. Protein Chem. 43*, 313−361.
43. Xie, D., and Freire, E. (1994) *J. Mol. Biol. 242*, 62−80.

BI992762G